

## Thermal stability of polycrystalline silicon electrodes on ZrO<sub>2</sub> gate dielectrics

Charles M. Perkins, Baylor B. Triplett, Paul C. McIntyre, Krishna C. Saraswat, and Eric Shero

Citation: [Applied Physics Letters](#) **81**, 1417 (2002); doi: 10.1063/1.1499513

View online: <http://dx.doi.org/10.1063/1.1499513>

View Table of Contents: <http://scitation.aip.org/content/aip/journal/apl/81/8?ver=pdfcov>

Published by the [AIP Publishing](#)

---

### Articles you may be interested in

[Thermal decomposition behavior of the HfO<sub>2</sub> / SiO<sub>2</sub> / Si system](#)

J. Appl. Phys. **94**, 928 (2003); 10.1063/1.1578525

[Interfacial properties of ZrO<sub>2</sub> on silicon](#)

J. Appl. Phys. **93**, 5945 (2003); 10.1063/1.1563844

[Thermal stability of polycrystalline silicon/metal oxide interfaces](#)

Appl. Phys. Lett. **81**, 4157 (2002); 10.1063/1.1526150

[Electrical characteristics and thermal stability of n + polycrystalline- Si/ZrO<sub>2</sub> /SiO<sub>2</sub> /Si metal-oxide-semiconductor capacitors](#)

J. Appl. Phys. **91**, 414 (2002); 10.1063/1.1425073

[Thermal stability of ultrathin ZrO<sub>2</sub> films prepared by chemical vapor deposition on Si\(100\)](#)

Appl. Phys. Lett. **78**, 368 (2001); 10.1063/1.1339994

---

Confidently measure down to 0.01 fA and up to 10 PΩ

Keysight B2980A Series Picoammeters/Electrometers

[View video demo](#)

A photograph of the Keysight B2980A Series Picoammeters/Electrometers, which is a small, handheld electronic device with a screen and various buttons.The Keysight Technologies logo, featuring a stylized red wave icon followed by the text "KEYSIGHT TECHNOLOGIES" in black.

## Thermal stability of polycrystalline silicon electrodes on ZrO<sub>2</sub> gate dielectrics

Charles M. Perkins, Baylor B. Triplett, and Paul C. McIntyre<sup>a)</sup>

*Department of Materials Science and Engineering, Stanford University, Stanford, California 94305*

Krishna C. Saraswat

*Department of Electrical Engineering, Stanford University, Stanford, California 94305*

Eric Shero

*ASM America, 3440 East University Drive, Phoenix, Arizona 85034*

(Received 10 December 2001; accepted for publication 15 June 2002)

Thermal stability of gate stack structures composed of ZrO<sub>2</sub> gate dielectrics and silicon electrodes was investigated. The ZrO<sub>2</sub> films were deposited by atomic layer deposition, while the polycrystalline silicon electrodes were deposited using different variants of chemical (CVD) and physical vapor deposition (PVD). Zirconium silicide formation was noted in all CVD-electroded samples after subsequent annealing treatments at temperatures above 750 °C, but not in the room temperature PVD-electroded samples, even after gate annealing at 1050 °C. The dependence of zirconium silicide formation on the Si deposition process was explained using thermodynamic arguments which explicitly include the effects of oxygen deficiency of the metal oxide films.

© 2002 American Institute of Physics. [DOI: 10.1063/1.1499513]

High- $\kappa$  metal oxides have been extensively studied as alternative gate dielectric materials to SiO<sub>2</sub> in metal-oxide-semiconductor devices beyond the 100 nm technology node.<sup>1</sup> Because dual metal gate electrode replacements impose additional processing complexities and limitations on operating voltages,<sup>2</sup> conventional polycrystalline silicon (poly-Si) remains an interesting gate electrode material. Recently, HfO<sub>2</sub> has emerged as a promising gate dielectric replacement due to its high dielectric constant and superior thermal stability in contact with Si-based electrodes.<sup>3</sup> Similar stability has been reported for ZrO<sub>2</sub> in certain special cases; for example, with a diffusion barrier between the ZrO<sub>2</sub> and silicon electrode.<sup>4</sup> In this letter, we demonstrate the thermal stability of the Si/SiO<sub>2</sub>/ZrO<sub>2</sub>/Si system under conventional dopant activation conditions without a barrier layer and show how stability of the poly-Si/ZrO<sub>2</sub> interface depends on the temperature and oxygen activity of the poly-Si growth process.

Uniform ultrathin (~50 Å) zirconium oxide films were deposited on 200 mm *p*-epi/*p*<sup>+</sup> silicon test wafers by atomic layer deposition (ALD) at ASM America Inc., using alternating surface-saturating reactions of ZrCl<sub>4</sub> and H<sub>2</sub>O at 300 °C. The ZrO<sub>2</sub> films in the first two of three test groups were deposited directly onto the original chemical silicon oxide of the as-received wafers. Films in the third test group were deposited onto an ultrathin (~15 Å) SiO<sub>2</sub> film grown by rapid thermal oxidation. The first test group utilized atmospheric chemical vapor deposition (CVD) to grow 1500 Å silicon films on the ZrO<sub>2</sub> films using SiH<sub>4</sub> and H<sub>2</sub> carrier gas (>10 SLM) at 620 °C. Deposition times were approximately 1–2 min. Low-pressure CVD was performed in a vertical furnace for samples in the second test group to deposit 500 Å silicon films using pure SiH<sub>4</sub> or Si<sub>2</sub>H<sub>6</sub> at 510 and 440 °C, respectively, at a pressure of a few Torr. Deposition times

were 60 to 90 min. Samples from the third test group were capped by 800 Å poly-Si films deposited by room temperature physical vapor deposition (PVD). The sputtering process utilized a lightly boron-doped silicon target and a base pressure of approximately 10<sup>-7</sup> Torr. Deposition times were several minutes with a 3–4 h pump down period.

After depositing the poly-Si films, the atmospheric CVD samples were annealed in a horizontal furnace using reagent grade N<sub>2</sub> gas. Temperatures ranged from 700 to 1000 °C while dwell times were kept constant at 1 h. Annealing of the low-pressure CVD and PVD samples utilized a rapid thermal annealer (RTA) and reagent grade N<sub>2</sub> gas. Temperatures were varied between 700 and 1050 °C with the dwell times of 5 s to 3 min. Cross sections of the gate stacks were examined by high-resolution transmission electron microscopy (TEM) using a Philips CM20 microscope operating at 200 kV. Crystalline phases within the gate stack were also monitored and indexed by selected area electron diffraction (SAD) of plan view samples.

Figure 1 shows high-resolution cross-sectional TEM images of a Si/SiO<sub>x</sub>/ZrO<sub>2</sub>/Si gate stack with a top silicon electrode deposited by atmospheric CVD using SiH<sub>4</sub> at 620 °C. Fast Fourier transforms were performed on both cross-sectional micrographs to determine the interplanar spacings of the different polycrystalline regions. The majority of the ZrO<sub>2</sub> film was indexed as tetragonal while a small percentage of the film exhibited diffraction features characteristic of the monoclinic phase. The silicide grains in both images were indexed as the orthorhombic ZrSi<sub>2</sub> phase. To analyze a more statistically significant sample area, SAD patterns were recorded using a SAD aperture that included a diffracting area of ~2 μm<sup>2</sup>. A representative electron diffraction ring pattern of the as-deposited sample is shown in Fig. 2(a). The only rings not indexed to tetragonal ZrO<sub>2</sub> interplanar spacings were indexed to the ZrSi<sub>2</sub> phase. The most intense (131)

<sup>a)</sup>Electronic mail: pcm1@leland.stanford.edu

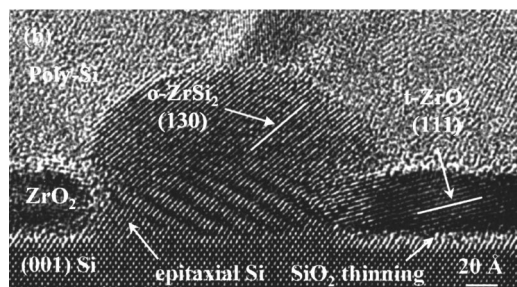
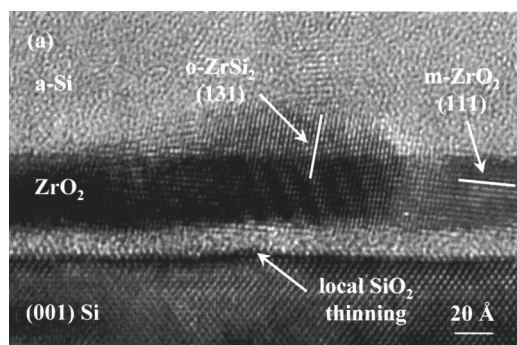


FIG. 1. Cross-sectional TEM images of a Si/SiO<sub>x</sub>/ZrO<sub>2</sub>/Si gate stack utilizing a 620 °C SiH<sub>4</sub> CVD process (a) as-deposited and (b) after a subsequent 1 h N<sub>2</sub> furnace anneal at 850 °C.

ZrSi<sub>2</sub> reflection was used to determine the occurrence of silicide formation in all samples in this study. The cross-sectional micrograph of the as-deposited gate stack also shows a local thinning of the SiO<sub>2</sub>-based interfacial layer beneath the silicide grain. The degree of thinning increased and was observed to spread to regions that were not in the immediate vicinity of a silicide particle during the subsequent high-temperature anneal. Epitaxial growth of silicon at the Si (100) wafer interface is also evident in the annealed sample around the sides of the silicide grain in Fig. 1(b), suggesting diffusion of silicon from the decomposing SiO<sub>2</sub> into the Si wafer during the anneal. It should be noted that high temperature N<sub>2</sub> annealing of bare (unelectroded) ZrO<sub>2</sub> films did not result in detectable ZrSi<sub>2</sub> formation.

A second set of CVD poly-Si deposition experiments explored the effects of lower thermal budgets and different silicon precursors on ZrSi<sub>2</sub> formation. Figure 2(b) is a representative SAD pattern of the as-deposited Si<sub>2</sub>H<sub>6</sub> sample. As with the as-deposited low temperature SiH<sub>4</sub> samples, no silicide diffraction signatures were observed; all detected rings were indexed to tetragonal ZrO<sub>2</sub>. Cross-sectional TEM images corroborated these results, showing no zirconium sil-

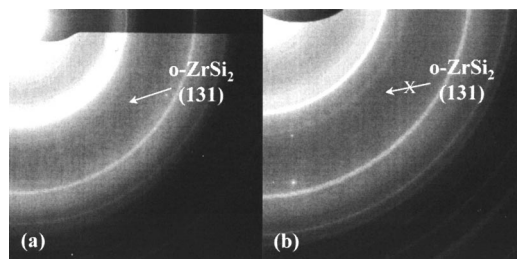


FIG. 2. SAD patterns of as-deposited samples show (a) ZrSi<sub>2</sub> diffraction signatures with the 620 °C SiH<sub>4</sub> CVD process and (b) thermal stability of the 510 °C SiH<sub>4</sub> CVD sample.

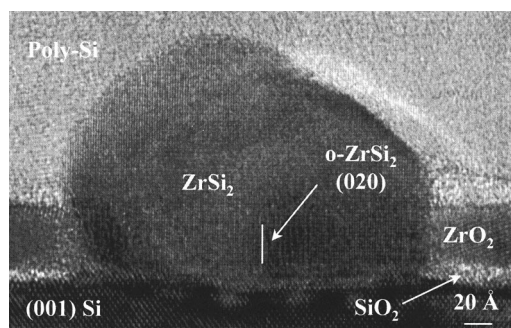


FIG. 3. Cross-sectional TEM micrograph illustrates a ZrSi<sub>2</sub> grain in a 510 °C SiH<sub>4</sub> CVD sample after a 1050 °C N<sub>2</sub> anneal.

icide particles or detectable thinning of the SiO<sub>2</sub> layer. Upon subsequent annealing, the Si<sub>2</sub>H<sub>6</sub> samples exhibited the best thermal stability, as silicide diffraction signatures were not observed below 800 °C. As illustrated in Fig. 3 for a low-temperature SiH<sub>4</sub> sample annealed at 1050 °C, higher temperature post-deposition anneals were again found to significantly thin the interfacial layer and cause silicon to diffuse to the base of the silicide grains.

The extent of silicide growth depended upon the post-electrode annealing temperature. Recent x-ray photoelectron spectroscopy studies reported thermal stability up to 900 °C for the Si/SiO<sub>2</sub>/ZrO<sub>2</sub>/Si system.<sup>5,6</sup> Because the initial onset of silicidation is a sparse and localized phenomenon, this technique may not be sensitive enough to detect the initial precipitates until their volume fraction in the gate stack reaches a few atomic percent. As a result, the onset of thermal instability in these previous studies<sup>5,6</sup> actually may have occurred at lower temperatures, similar to those reported in this paper.

A third set of samples was fabricated using a room temperature sputtering process to deposit the poly-Si gate electrode (Fig. 4). Unlike the samples made using CVD methods, the PVD material was stable with respect to ZrSi<sub>2</sub> formation at temperatures up to those of conventional dopant activation anneals. Thinning of the interfacial layer was observed after the anneal.

Several groups have suggested that the observed silicidation during vacuum annealing of uncapped ZrO<sub>2</sub> films results from SiO evaporation which decomposes the SiO<sub>2</sub> layer and removes oxygen from the ZrO<sub>2</sub>.<sup>5,7</sup> Oxygen loss by SiO evaporation is well established for thin SiO<sub>2</sub> films for temperatures between 700 and 1000 °C.<sup>8,9</sup> Reduction of the zirconia films to form oxygen-deficient ZrO<sub>2-x</sub> by loss of molecular oxygen during the early stages of poly-Si deposition

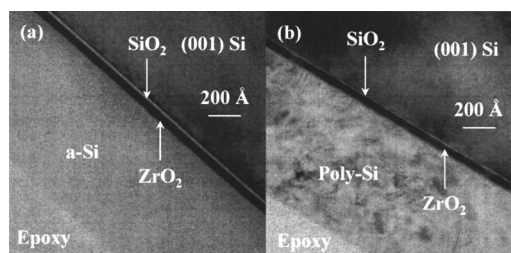


FIG. 4. Cross-sectional TEM micrographs of a Si/SiO<sub>x</sub>/ZrO<sub>2</sub>/Si gate stack utilizing a room temperature PVD process in both the (a) as-deposited condition and (b) after a 10 s N<sub>2</sub> RTA step at 1050 °C.



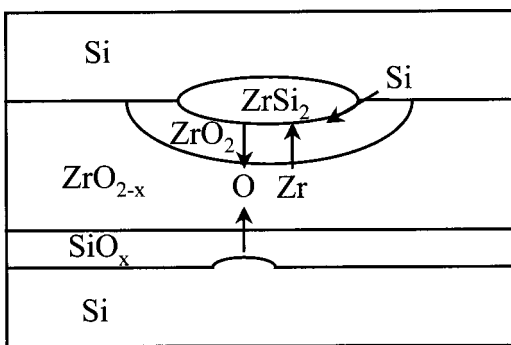
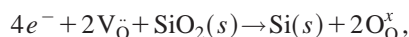


FIG. 5. The proposed process of silicidation involves (1) decomposition of  $\text{ZrO}_2$ , (2) Zr diffusion and reaction with Si to form  $\text{ZrSi}_2$ , and (3) O diffusion and filling of oxygen vacancies in  $\text{ZrO}_{2-x}$  regions. Note concurrent O diffusion from the  $\text{SiO}_2$  layer.

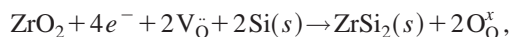
is also possible. The poly-Si CVD precursor ambients (e.g.,  $\text{H}_2/\text{SiH}_4$ ) are expected to have extremely low oxygen activity. As a result, it is reasonable that oxygen loss should occur (perhaps involving SiO) during the initial phases of silicon deposition given the tendency of  $\text{ZrO}_2$  to become oxygen deficient.<sup>12</sup> In this study, thinning of the interfacial layer was not observed in the lower temperature (440–510 °C) CVD and the PVD samples until after post-electrode annealing. Once a thick Si layer caps the  $\text{ZrO}_2$  film, exchange of oxygen between the sample and the ambient is kinetically inhibited. Therefore, continual SiO evaporation<sup>5,7</sup> cannot account for the observed silicidation and  $\text{SiO}_2$  thinning during post-electrode anneals.

The elevated temperatures and low oxygen activity of conventional CVD silicon deposition may create oxygen vacancies in the  $\text{ZrO}_2$ , in addition to oxygen vacancies present in the as-deposited metal oxide films. Reported thermodynamic data suggest that there is a driving force for oxygen exchange between oxygen deficient  $\text{ZrO}_2$  and  $\text{SiO}_2$  via the following reaction (using Kröger-Vink notation)<sup>12</sup>



where the individual processes can be thought off as: (1) decomposition of  $\text{SiO}_2$  into its elemental constituents and (2) filling of oxygen vacancies in  $\text{ZrO}_2$ . The enthalpy change of the combined process is predicted to be large and negative ( $\sim -230$  kJ/mol).<sup>10,11</sup> As this is a solid state reaction, the entropy change is relatively small and the enthalpy change should accurately represent the total driving force for thinning of the interfacial  $\text{SiO}_2$  layer.

We propose that the process of silicidation is also dependent on the oxygen stoichiometry of the  $\text{ZrO}_2$  layer after silicon deposition. Oxygen deficiency of the  $\text{ZrO}_2$  films may cause  $\text{ZrSi}_2$  formation to become energetically favorable. This is summarized (see Fig. 5) by the reaction



which can be thought of as to the summation of three processes: (1) decomposition of  $\text{ZrO}_2$  into its elemental constituents, (2) reaction between the resulting metallic Zr and Si to form  $\text{ZrSi}_2$ , and (3) filling of two oxygen vacancies in a nonstoichiometric area of the  $\text{ZrO}_2$  film. The enthalpy

change of the combined process is also large and negative ( $\sim -190$  kJ/mol),<sup>10–12</sup> indicating a large driving force for zirconium silicide formation from oxygen deficient  $\text{ZrO}_2$  via this solid state reaction.

Although the predicted driving forces for  $\text{SiO}_2$  decomposition and  $\text{ZrSi}_2$  formation at the  $\text{ZrO}_{2-x}/\text{SiO}_{2-x}$  and  $\text{Si}/\text{ZrO}_{2-x}$  interfaces, respectively, are not dissimilar, our annealing experiments on PVD poly-Si electroded samples showed a complete absence of silicidation but a detectable  $\text{SiO}_2$  thinning. This suggests that the ALD  $\text{ZrO}_2$  films were somewhat oxygen deficient as-deposited and that the PVD poly-Si deposition process did not add to this initial oxygen nonstoichiometry. Furthermore, one expects a substantial kinetic barrier to nucleation of the silicide particles associated with formation of  $\text{Si}/\text{ZrSi}_2$  and  $\text{ZrSi}_2/\text{ZrO}_2$  interfaces. No new interfaces are needed for  $\text{SiO}_2$  thinning to take place. The elevated temperature of the CVD processes may promote formation of  $\text{ZrSi}_2$  nuclei at the poly-Si/ $\text{ZrO}_2$  interface. These nuclei would then grow during post-electrode anneals, consistent with the observed particle formation during annealing of the CVD samples.

In summary, we have demonstrated a correlation between poly-Si gate electrode deposition conditions and the silicidation of  $\text{ZrO}_2$  gate dielectrics, whereby high deposition temperatures and reducing CVD ambients encourage formation of  $\text{ZrSi}_2$  particles. We have also shown that  $\text{ZrSi}_2$  formation occurs during postelectrode annealing of  $\text{ZrO}_2$  samples that are capped by a thick, continuous poly-Si electrode layer, when the electrode deposition occurs under typical CVD conditions. These results are consistent with thermodynamically favored processes in which oxygen vacancies present in the  $\text{ZrO}_2$  dielectric are annihilated through  $\text{SiO}_2$  decomposition and  $\text{ZrSi}_2$  formation.

This work was supported in part by the NSF/SRC Engineering Research Center for Environmentally Benign Semiconductor Manufacturing and Intel Corporation.

<sup>1</sup> Semiconductor Industry Association, *The International Technology Roadmap for Semiconductors* (Sematech, Austin, 2000).

<sup>2</sup> Y. Abe, T. Oishi, K. Shiozawa, Y. Tokuda, and S. Satoh, *IEEE Electron Device Lett.* **20**, 632 (1999).

<sup>3</sup> B. Ricco, R. Vesari, and D. Esseni, *IEEE Electron Device Lett.* **17**, 103 (1996).

<sup>4</sup> S. J. Lee, H. F. Luan, W. P. Bai, C. H. Lee, T. S. Jeon, Y. Senzaki, D. Roberts, and D. L. Kwong, *Tech. Dig. Int. Electron Devices Meet.* **2000**, 31 (2000).

<sup>5</sup> T. S. Jeon, J. M. White, and D. L. Kwong, *Appl. Phys. Lett.* **78**, 368 (2001).

<sup>6</sup> C. H. Lee, H. F. Luan, W. P. Bai, S. J. Lee, T. S. Jeon, Y. Senzaki, D. Roberts, and D. L. Kwong, *Tech. Dig. Int. Electron Devices Meet.* **2000**, 27 (2000).

<sup>7</sup> J.-P. Maria, D. Wicaksana, A. I. Kingon, B. Busch, H. Schulte, E. Garfunkel, and T. Gustafsson, *J. Appl. Phys.* **90**, 3476 (2001).

<sup>8</sup> R. Tromp, G. W. Rubloff, P. Balk, F. K. LeGoues, and E. J. van Loenen, *Phys. Rev. Lett.* **55**, 2332 (1985).

<sup>9</sup> N. Miyata, H. Watanabe, and M. Ichikawa, *Phys. Rev. Lett.* **84**, 1043 (2000).

<sup>10</sup> I. Barin and O. Knacke, *Thermochemical Properties of Inorganic Substances* (Springer, Berlin, 1973).

<sup>11</sup> I. Barin, *Thermochemical Data of Pure Substances*, 3rd ed. (VCH, New York, 1995), Vol. 2.

<sup>12</sup> W.-E. Wang and D. R. Olander, *J. Am. Ceram. Soc.* **76**, 1242 (1993).